arXiv:hep-ex/0605105v1 24 May 2006

Measurements of the cross sections for $e^+e^- \to$ hadrons at 3.650, 3.6648, 3.773 GeV and the branching fraction for $\psi(3770) \to$ non$-D\bar{D}$

M. Ablikim[1], J. Z. Bai[1], Y. Ban[11], J. G. Bian[1], X. Cai[1], H. F. Chen[15], H. S. Chen[1], H. X. Chen[1], J. C. Chen[1], Jin Chen[1],
Y. B. Chen[1], S. P. Chi[2], Y. P. Chu[1], X. Z. Cui[1], Y. S. Dai[17], Z. Y. Deng[1], L. Y. Dong[1a], Q. F. Dong[14], S. X. Du[1], Z. Z. Du[1],
J. Fang[1], S. S. Fang[2], C. D. Fu[1], C. S. Gao[1], Y. N. Gao[14], S. D. Gu[1], Y. T. Gu[4], Y. N. Guo[1], Y. Q. Guo[1], K. L. He[1],
M. He[12], Y. K. Heng[1], H. M. Hu[1], T. Hu[1], X. P. Huang[1], X. T. Huang[12], X. B. Ji[1], X. S. Jiang[1], J. B. Jiao[12], D. P. Jin[1],
S. Jin[1], Yi Jin[1], Y. F. Lai[1], G. Li[2], H. B. Li[1], H. H. Li[1], J. Li[1], R. Y. Li[1], S. M. Li[1], W. D. Li[1], W. G. Li[1], X. L. Li[8],
X. Q. Li[10], Y. L. Li[4], Y. F. Liang[13], H. B. Liao[6], C. X. Liu[1], F. Liu[6], Fang Liu[15], H. H. Liu[1], H. M. Liu[1], J. Liu[11], J. B. Liu[1],
J. P. Liu[16], R. G. Liu[1], Z. A. Liu[1], F. Lu[1], G. R. Lu[5], H. J. Lu[15], J. G. Lu[1], C. L. Luo[9], F. C. Ma[8], H. L. Ma[1], L. L. Ma[1],
Q. M. Ma[1], X. B. Ma[5], Z. P. Mao[1], X. H. Mo[1], J. Nie[1], H. P. Peng[15], N. D. Qi[1], H. Qin[9], J. F. Qiu[1], Z. Y. Ren[1], G. Rong[1],
L. Y. Shan[1], L. Shang[1], D. L. Shen[1], X. Y. Shen[1], H. Y. Sheng[1], F. Shi[1], X. Shi[11b], H. S. Sun[1], J. F. Sun[1], S. S. Sun[1],
Y. Z. Sun[1], Z. J. Sun[1], Z. Q. Tan[4], X. Tang[1], Y. R. Tian[14], G. L. Tong[1], D. Y. Wang[1], L. Wang[1], L. S. Wang[1],
M. Wang[1], P. Wang[1], P. L. Wang[1], W. F. Wang[1c], Y. F. Wang[1], Z. Wang[1], Z. Y. Wang[1], Zhe Wang[1], Zheng Wang[2],
C. L. Wei[1], D. H. Wei[1], N. Wu[1], X. M. Xia[1], X. X. Xie[1], B. Xin[8d], G. F. Xu[1], Y. Xu[10], M. L. Yan[15], F. Yang[10],
H. X. Yang[1], J. Yang[15], Y. X. Yang[3], M. H. Ye[2], Y. X. Ye[15], Z. Y. Yi[1], G. W. Yu[1], C. Z. Yuan[1], J. M. Yuan[1], Y. Yuan[1],
S. L. Zang[1], Y. Zeng[7], Yu Zeng[1], B. X. Zhang[1], B. Y. Zhang[1], C. C. Zhang[1], D. H. Zhang[1], H. Y. Zhang[1], J. W. Zhang[1],
J. Y. Zhang[1], Q. J. Zhang[1], X. M. Zhang[1], X. Y. Zhang[12], Yiyun Zhang[13], Z. P. Zhang[15], Z. Q. Zhang[5], D. X. Zhao[1],
J. W. Zhao[1], M. G. Zhao[1], P. P. Zhao[1], W. R. Zhao[1], H. Q. Zheng[11], J. P. Zheng[1], Z. P. Zheng[1], L. Zhou[1], N. F. Zhou[1],
K. J. Zhu[1], Q. M. Zhu[1], Y. C. Zhu[1], Y. S. Zhu[1], Yingchun Zhu[1e], Z. A. Zhu[1], B. A. Zhuang[1], X. A. Zhuang[1], B. S. Zou[1]
(BES Collaboration)
[1] *Institute of High Energy Physics, Beijing 100049, People's Republic of China*
[2] *China Center for Advanced Science and Technology(CCAST), Beijing 100080, People's Republic of China*
[3] *Guangxi Normal University, Guilin 541004, People's Republic of China*
[4] *Guangxi University, Nanning 530004, People's Republic of China*
[5] *Henan Normal University, Xinxiang 453002, People's Republic of China*
[6] *Huazhong Normal University, Wuhan 430079, People's Republic of China*
[7] *Hunan University, Changsha 410082, People's Republic of China*
[8] *Liaoning University, Shenyang 110036, People's Republic of China*
[9] *Nanjing Normal University, Nanjing 210097, People's Republic of China*
[10] *Nankai University, Tianjin 300071, People's Republic of China*
[11] *Peking University, Beijing 100871, People's Republic of China*
[12] *Shandong University, Jinan 250100, People's Republic of China*
[13] *Sichuan University, Chengdu 610064, People's Republic of China*
[14] *Tsinghua University, Beijing 100084, People's Republic of China*
[15] *University of Science and Technology of China, Hefei 230026, People's Republic of China*
[16] *Wuhan University, Wuhan 430072, People's Republic of China*
[17] *Zhejiang University, Hangzhou 310028, People's Republic of China*
[a] *Current address: Iowa State University, Ames, IA 50011-3160, USA*
[b] *Current address: Cornell University, Ithaca, NY 14853, USA*
[c] *Current address: Laboratoire de l'Accélératear Linéaire, Orsay, F-91898, France*
[d] *Current address: Purdue University, West Lafayette, IN 47907, USA*
[e] *Current address: DESY, D-22607, Hamburg, Germany*

Using the BES-II detector at the BEPC Collider, we measured the lowest order cross sections and the R values ($R = \sigma^0_{e^+e^-\to \mathrm{hadrons}}/\sigma^0_{e^+e^-\to\mu^+\mu^-}$) for inclusive hadronic event production at the center-of-mass energies of 3.650 GeV, 3.6648 GeV and 3.773 GeV. The results lead to $\bar{R}_{uds} = 2.224 \pm 0.019 \pm 0.089$ which is the average of these measured at 3.650 GeV and 3.6648 GeV, and $R = 3.793 \pm 0.037 \pm 0.190$ at $\sqrt{s} = 3.773$ GeV. We determined the lowest order cross section for $\psi(3770)$ production to be $\sigma^{\mathrm{B}}_{\psi(3770)} = (9.575 \pm 0.256 \pm 0.813)$ nb at 3.773 GeV, the branching fractions for $\psi(3770)$ decays to be $BF(\psi(3770) \to D^0\bar{D}^0) = (48.9 \pm 1.2 \pm 3.8)\%$, $BF(\psi(3770) \to D^+D^-) = (35.0 \pm 1.1 \pm 3.3)\%$ and $BF(\psi(3770) \to D\bar{D}) = (83.9 \pm 1.6 \pm 5.7)\%$, which result in the total non-$D\bar{D}$ branching fraction of $\psi(3770)$ decay to be $BF(\psi(3770) \to \mathrm{non}-D\bar{D}) = (16.1 \pm 1.6 \pm 5.7)\%$.

I. INTRODUCTION

proceeds via quark-antiquark pair production where the photon couples directly to the charge of the pointlike quarks. A consequence of this picture is that the total lowest order cross section, $\sigma^{\rm B}_{had}$, for inclusive hadron production in e^+e^- annihilation must be proportional to the lowest order cross section, $\sigma^{\rm B}_{\mu^+\mu^-}$, for muon pair production, which results in the relation

$$\sigma^{\rm B}_{\rm had} = 3\sum_i^{N_f} Q_i^2 \ \sigma^{\rm B}_{\mu^+\mu^-}, \qquad (1)$$

where Q_i is the charge of the ith quark; the factor of 3 accounts for three different colors of quarks; the sum runs over all quark flavors, N_f, involved, for which the quark pair production thresholds are below the e^+e^- annihilation energy. The Eq. (1) indicates the ratio

$$R = \frac{\sigma^{\rm B}_{\rm had}}{\sigma^{\rm B}_{\mu^+\mu^-}} = 3\sum_i^{N_f} Q_i^2 \qquad (2)$$

to be constant as long as the c.m. (center-of-mass) energy E_{cm} does not overlap with resonances or the threshold of the production of new quark flavors. It also indicates that the R_{uds} value for continuum light hadron (containing u, d and s quarks) production should tend to be constant in the energy region above 2 GeV.

This naive theoretical prediction for the R value has to be modified to take into account the finite mass of the quarks and the emission of the gluons by the quarks. In principle, the R values can be computed in the pQCD (perturbative QCD) with these corrections. So precise measurements of R values at low energy region are important for the test of the prediction by the pQCD in this energy region. Moreover the R values at all energies are needed to calculate the effects of vacuum polarization on the parameters of the Standard Model. For example, the dominant uncertainties in the quantities $\alpha(M_Z^2)$, the QED running coupling constant evaluated at the mass of Z^0, and $a_\mu = (g-2)/2$, the anomalous magnetic moment of the muon, are due to the calculation of hadronic vacuum polarization[1]. A large part of uncertainty in the calculation arises from the uncertainties in the measured inclusive hadronic cross sections in open charm threshold region, in which many resonances overlap. To get credible measurements of R and various lowest order cross sections in this region, the overlapping effects have to be clarified clearly.

On the other hand, the measurements of the R values below and above the threshold of $D\bar{D}$ production can be used to determine the branching fractions for $\psi(3770) \to D^0\bar{D}^0, D^+D^-, D\bar{D}$, and for $\psi(3770) \to$ non$-D\bar{D}$ with the measured cross sections for the $D^0\bar{D}^0$ and D^+D^- together. The $\psi(3770)$ resonance is believed to decay predominantly into $D\bar{D}$ [2]. However, there are discrepancies between the measurements of the $D\bar{D}$ cross section and the measurements of $\psi(3770)$ cross section which can be obtained from $\psi(3770)$ resonance parameters. In recent days, there are some publications to report the observation of non$-D\bar{D}$ decays of $\psi(3770)$ resonance [3][4][5]. In this Letter, we present more precise measurements of the R values at the c.m. energies of 3.650, 3.6648 and 3.773 GeV. With the measured R values and the previously measured cross sections for $D\bar{D}$ production at 3.773 GeV [6], we determine the branching fractions for $\psi(3770) \to D^0\bar{D}^0, D^+D^-, D\bar{D}$, and for $\psi(3770) \to$ non$-D\bar{D}$

II. BES-II DETECTOR

The BES-II is a conventional cylindrical magnetic detector that is described in detail in Ref. [7]. A 12-layer Vertex Chamber (VC) surrounding the beryllium beam pipe provides input to the event trigger, as well as coordinate information. A forty-layer main drift chamber (MDC) located just outside the VC yields precise measurements of charged particle trajectories with a solid angle coverage of 85% of 4π; it also provides ionization energy loss (dE/dx) measurements which are used for particle identification. Momentum resolution of $1.7\%\sqrt{1+p^2}$ (p in GeV/c) and dE/dx resolution of 8.5% for Bhabha scattering electrons are obtained for the data taken at $\sqrt{s} = 3.773$ GeV. An array of 48 scintillation counters surrounding the MDC measures the time of flight (TOF) of charged particles with a resolution of about 180 ps for electrons. Outside the TOF, a 12 radiation length, lead-gas barrel shower counter (BSC), operating in limited streamer mode, measures the energies of electrons and photons over 80% of the total solid angle with an energy resolution of $\sigma_E/E = 0.22/\sqrt{E}$ (E in GeV) and spatial resolutions of $\sigma_\phi = 7.9$ mrad and $\sigma_Z = 2.3$ cm for electrons. A solenoidal magnet outside the BSC provides a 0.4 T magnetic field in the central tracking region of the detector. Three double-layer muon counters instrument the magnet flux return and serve to identify muons with momentum greater than 500 MeV/c. They cover 68% of the total solid angle.

III. MEASUREMENT OF THE OBSERVED HADRONIC CROSS SECTIONS

For a sample of data taken at c.m. energy $E_{{\rm cm},i}$, the observed cross section for the inclusive hadronic event production is obtained by

$$\sigma^{\rm obs}(E_{{\rm cm},i}) = \frac{N_{\rm had}(E_{{\rm cm},i})}{L(E_{{\rm cm},i}) \ \epsilon_{\rm had}(E_{{\rm cm},i}) \ \epsilon^{\rm trig}_{\rm had}}, \qquad (3)$$

where i is the ith energy point at which the data were collected, $N_{\rm had}(E_{{\rm cm},i})$ is the number of the inclusive hadronic events observed at this energy; $L(E_{{\rm cm},i})$ is the integrated luminosity of the data collected; $\epsilon_{\rm had}(E_{{\rm cm},i})$ is the efficiency for detection of the inclusive hadronic events, and $\epsilon^{\rm trig}_{\rm had}$ is the trigger efficiency for collecting the hadronic events in on-line data acquisition.

A. Measurement of luminosity

The integrated luminosities of the data sets are determined by

$$L(E_{\rm cm,\it i}) = \frac{N_{e^+e^-}(E_{\rm cm,\it i}) - n_b}{\sigma_{e^+e^-}(E_{\rm cm,\it i})\ \epsilon_{e^+e^-}(E_{\rm cm,\it i})\ \epsilon^{\rm trig}_{e^+e^-}}, \tag{4}$$

where $N_{e^+e^-}(E_{cm,i})$ and n_b are the number of the selected Bhabha events and the number of background events respectively, $\epsilon_{e^+e^-}(E_{cm,i})$ is the efficiency for detection of the Bhabha events, $\epsilon^{\rm trig}_{e^+e^-}$ is the trigger efficiency for collecting the Bhabha events in on-line data acquisition. For the data used in the analysis, the trigger efficiency is $\epsilon^{\rm trig}_{e^+e^-} = (100.0^{+0.0}_{-0.5})\%$ (see subsection D).

To select the candidates for Bhabha scattering $e^+e^- \to (\gamma)e^+e^-$, it is first required that exactly two charged tracks with total charge zero be well reconstructed. For each track, the point of the closest approach to the beam line must have the radius $\leq$ 1.5 cm and $|z| \leq$ 15 cm where $|z|$ is measured along the beam line from the nominal beam crossing point. Furthermore, each track is required to satisfy $|\cos\theta| \leq 0.7$, where θ is the polar angle of the charged track, to ensure that it is contained within the barrel region of the detector. Next, it is required that the energy deposited for each charged track in BSC be greater than 1.1 GeV (i.e. $E^{\rm track}_{\rm BSC} > 1.1$ GeV) and at least the magnitude of one charged track momentum be greater than $0.9E_{\rm b}$, where $E_{\rm b}$ is the beam energy. Figure 1 shows the distribution of the energies deposited for muons (hatched histogram) and electrons or positrons (points with error bars) in the BSC, where the data sample of the muons and the electrons or positrons are selected from the decays of $\psi(2S) \to J/\psi\pi^+\pi^-$, and $J/\psi \to \mu^+\mu^-$ or e^+e^-. From Fig. 1 one can see that the criterion $E^{\rm track}_{\rm BSC} > 1.1$ GeV separates the $e^+e^- \to (\gamma)\mu^+\mu^-$ from the Bhabha scattering effectively. In addition, because the Monte Carlo simulation does not model the energy deposited well in the rib regions of the BSC, any charged track from the selected Bhabha events is required to hit one of the four regions of the BSC (selected z regions in BSC): (1) $z_{\rm BSC} \leq -1.04$ m, (2) -0.77 m $\leq z_{\rm BSC} \leq -0.1$ m, (3) 0.1 m $\leq z_{\rm BSC} \leq 0.77$ m, (4) $z_{\rm BSC} \geq 1.04$ m.

The two oppositely charged tracks go in opposite directions in the $R-\phi$ plane. Because the tracks are bent in the magnetic field, the positions of the two shower clusters in the $R-\phi$ plane of the BSC are deviated from the back-to-back directions. We define the angle difference of the two clusters by $\delta\phi = |\phi_1 - \phi_2| - 180^o$ in degrees, where the ϕ_1 and ϕ_2 are the azimuthal angles of the two clusters in the BSC. Figure 2 shows the $\delta\phi$ distribution for the events which satisfy the selection criteria for the Bhabha events. These events are from a portion of the data taken at 3.773 GeV. Using a double Gaussian function plus a second order polynomial to fit the distribution, we obtain the number of the candidates for $e^+e^- \to (\gamma)e^+e^-$. The accepted candidate events are examined for background contaminations by visual scan. The detailed scans for the accepted $e^+e^- \to (\gamma)e^+e^-$ events show that about 0.5% of the accepted events are due to background contamination. After subtracting the background, the pure number of $e^+e^- \to (\gamma)e^+e^-$ events is retained.

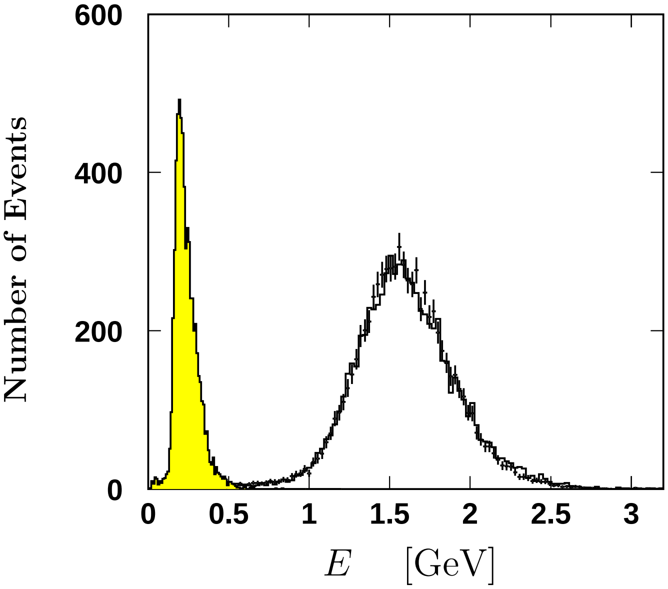

FIG. 1: The distribution of energies deposited for muons (hatched histogram) and electrons or positrons (points with error bars) in BSC, where the sample of the muons and the electrons or positrons is from the decays of $\psi(2S) \to J/\psi\pi^+\pi^-$, and $J/\psi \to \mu^+\mu^-$ or e^+e^-; the open histogram is for the electrons or positrons from the Monte Carlo events of $\psi(2S) \to J/\psi\pi^+\pi^-$, and $J/\psi \to e^+e^-$.

The detection efficiency $\epsilon_{e^+e^-}$ for the Bhabha scattering $e^+e^- \to (\gamma)e^+e^-$ is determined by analyzing the Monte Carlo events of $e^+e^- \to (\gamma)e^+e^-$. These events are generated with the radiative Bhabha generator [8] written by R. Kleiss *et al.*, which includes hard photon emission and α^3 radiative correction.

Using the pure number selected, the visible cross section $\sigma_{e^+e^-}$ read from the generator, the detection efficiency for $e^+e^- \to (\gamma)e^+e^-$ obtained by Monte Carlo simulation, and the trigger efficiency, we can determine the integrated luminosity of the data from Eq. (4). Applying the procedure to the data sets taken at the three energy points, we get the measured integrated luminosities of the data sets. The second column of table I lists the integrated luminosities of the data sets, where the errors are combined from statistical and systematic errors.

The systematic uncertainty in the measured values of the luminosities arises mainly from the difference between the data and Monte Carlo simulation. Table II summarizes the systematic uncertainties due to the $e^+e^- \to (\gamma)e^+e^-$ event selection criteria. The total uncertainty in the measured luminosity is estimated to be about 1.8%.

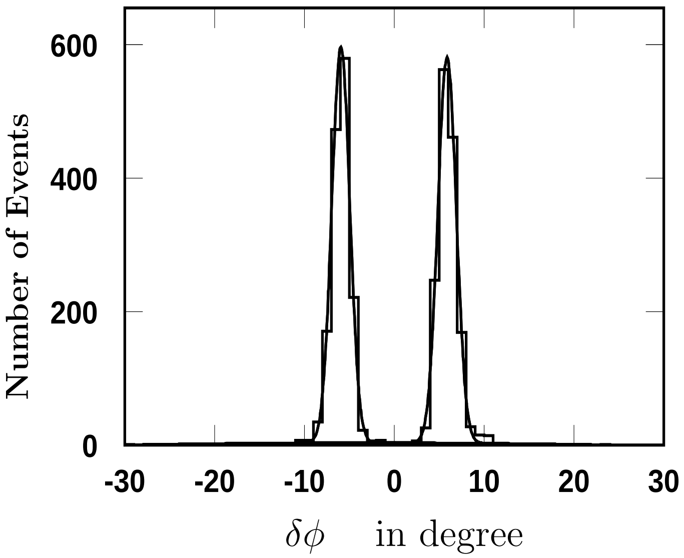

FIG. 2: The distribution of the $\delta\phi$ ($\delta\phi = |\phi_1 - \phi_2| - 180^o$) of the selected e^+ and e^- tracks.

TABLE I: Summary of the luminosities of the data sets, the numbers of the selected candidates for $e^+e^- \to$ *hadrons* and the estimated numbers of the events of the processes $e^+e^- \to l^+l^-$ ($l = \tau, e, \mu$), $e^+e^- \to e^+e^-l^+l^-$ and $e^+e^- \to e^+e^-$ *hadrons* which were misidentified as the events of $e^+e^- \to$ *hadrons*.

E_{cm}	L	$N_{\rm had}^{\rm zfit}$	$n_{l^+l^-}$	$n_{e^+e^-l^+l^-}$
(GeV)	[nb^{-1}]			& $n_{e^+e^-h}$
3.650	5537.7 ± 102.3	54576 ± 239	2038	219
3.6648	998.2$\pm$ 19.2	9615 ± 100	382	40
3.773	17300.0 ± 319.6	274021 ± 538	8603	701

B. Selection of hadronic events

In order to effectively remove the $e^+e^- \to (\gamma)e^+e^-$ and $e^+e^- \to (\gamma)\mu^+\mu^-$ events from the selected hadronic event sample, the hadronic events are required to have more than 2 good charged tracks, each of which is required to satisfy the following selection criteria:

- the charged track must be with a good helix fit and the number of dE/dx hits per charged track is required to be greater than 14;
- the point of the closest approach to the beam line must have radius ≤ 2.0 cm;
- $|\cos\theta| \leq 0.84$, where θ is the polar angle of the charged track;
- $p \leq E_b + 0.1 \times E_b \times \sqrt{(1+E_b^2)}$, where p is the charged track momentum and E_b is the beam energy in GeV;

TABLE II: The relative systematic uncertainties in the measured luminosity due to the $e^+e^- \to (\gamma)e^+e^-$ event selection criteria.

Criterion	$\frac{\Delta_L}{L}$ [%]
Radius < 1.5 cm	0.18
$\lvert z\rvert < 15$ cm	0.48
$\lvert cos\theta\rvert < 0.7$	0.65
$E_{\rm BSC}^{\rm track} > 1.1$ GeV	0.27
$P_+^{\rm track}$(or $P_-^{\rm track}$) $> 0.9E_{\rm b}$	1.33
Selected z regions in BSC	0.89
Total uncertainty in Bhabha event	1.83

- $2.0\ ns \leq T_{TOF} \leq T_p + 2.0\ ns$, where T_{TOF} is the time-of-flight of the charged particle, and T_p is the expected time-of-flight of proton with the given momentum;
- the charged track must not be identified as a muon;
- for the charged track, the energy deposited in BSC should be less than 1.0 GeV.

In addition, the total energy deposited in BSC should be greater than 28% of the beam energy. Furthermore, the selected tracks must not all point into the same hemisphere in the z direction. No criterion for the number of the observed photons is applied to the selected hadronic events.

Some beam-gas associated background events can also satisfy above selection criteria. However, the beam-gas associated background events are produced at random z positions, while the hadronic events are produced around $z = 0$. This characteristic can be used to distinguish the hadronic events from the beam-gas associated background events. To this end, the averaged z of the charged tracks in each event is calculated. Figure 3 shows the distribution of the averaged z. These events are from a portion of the data taken at 3.773 GeV. In Fig. 3, the points with error bars show the events from the Monte Carlo sample which is generated with the generator [9] described in Section III.C and simulated with the GEANT3-based Monte Carlo package [10], the histogram shows the events from the data, and the shadowed histogram shows the events from the separated beam data. Using a Gaussian function plus a second order polynomial to fit the averaged z distribution of the events, we obtain the number, $N_{\rm had}^{\rm zfit}$, of the candidates for hadronic events. The third column of table I lists $N_{\rm had}^{\rm zfit}$ obtained from the data sets taken at each of the energy points, where the errors are combined from statistical and systematic errors. This number of candidates contains some contaminations from some background events such as $e^+e^- \to \tau^+\tau^-$, $e^+e^- \to (\gamma)e^+e^-$, $e^+e^- \to (\gamma)\mu^+\mu^-$ and two-photon exchange processes. The number of the background events can be estimated by means of Monte Carlo simulation (see Section III.E).

TABLE III: The relative systematic uncertainties in measuring the produced hadronic events due to the event selection.

Criterion	$\Delta_{N^{\rm prd}_{\rm had}}/N^{\rm prd}_{\rm had}$ [%]
Good helix fit	0.10
$N_{dE/dx} > 14$	0.01
$V_{xy} < 0.02$ m	1.30
$\|cos\theta\| < 0.84$	0.36
$p < E_b + 0.1 \times E_b \times \sqrt{(1+E_b^2)}$	0.07
$2.0\ ns\ < T_{TOF} < T_p + 2.0\ ns$	0.43
μId = .false.	0.04
$E^{\rm TRK}_{\rm BSC} < 1.0$ GeV	0.56
$E_{\rm BSC} > 0.28E_{\rm b}$	0.49
Same hemisphere cut	1.01
Fitting to averaged Z distribution	0.65
$N_{\rm chtrk} \geq 3$	1.5
Total uncertainty	2.50

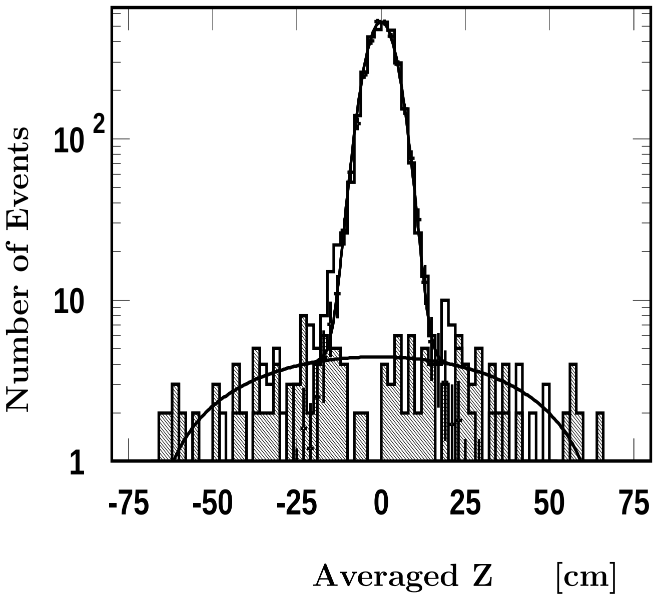

FIG. 3: The distribution of the averaged z of the charged tracks which satisfy the hadronic event selection criteria, where points with error bars show the events from the Monte Carlo sample, the histogram shows the events from the data, and the shadowed histogram shows the events from the separated beam data; the curves give the best fit to the z distribution.

The systematic uncertainty in measuring the produced hadronic events due to the hadronic event selection criteria is estimated to be about 2.5%. Table III summarizes the relative systematic uncertainties in selecting the produced hadronic events.

C. Monte Carlo method and the efficiency ϵ_{had}

Due to ISR (Initial State Radiation), the effective c.m. energy for the e^+e^- annihilation is $E_{\rm eff} = \sqrt{s(1-x)}$, where $x\sqrt{s}/2$ is the total energy of the emitted photons and $\sqrt{s}$ is the nominal c.m. energy. For a certain energy point in experiment, the experimentally observed hadronic events are not only produced at the $\sqrt{s}$, but produced in the full energy range from the $\sqrt{s}$ to ~ 0.28 GeV (for production of two pions). To determine the efficiency for detection of hadronic events produced in the full energy range, we developed a special Monte Carlo generator [9] in which the initial state radiative correction to α^2 order is taken into account.

Figure 4 shows the differential cross section $d\sigma/dE_{\rm eff}$ for the inclusive hadronic event production when setting the nominal c.m. energy to be at 3.80 GeV. At an effective c.m. energy, the final hadronic states are produced by calling the sub-generators such as LUND model [11][12], and the resonance generators including $\psi(3770)$, $\psi(2S)$, J/ψ [13], $\phi(1020)$, $\rho(770)$, and $\omega(782)$ etc. according to the corresponding lowest order cross sections of these processes, respectively. The CMD-2 $\pi\pi$ production data [14] with Gounaris-Sakurai parameterization [15] are used to simulate the spectrum of $\rho(770)$ and the ρ-ω mixing in the energy range below 1.2 GeV. The resonances are set to decay into all possible final states according to the known decay modes and branching fractions. These generated events are simulated with the GEANT3-based Monte Carlo simulation package. The reconstructed Monte Carlo events are then fed into the analysis program to determine the efficiencies, ϵ_{had}, for measurements of the observed cross sections for inclusive hadronic event production at each of the three energy points.

For simulations of the inclusive hadron production, parameters in the LUND generator are tuned using an inclusive hadronic event sample of 5.5×10^5 events from the data taken at 3.65 GeV with the BES-II detector. The parameters are adjusted to reproduce good agreeable distributions of some main kinematic variables between data and Monte Carlo sample. The uncertainty in ϵ_{had} due to the adjusted parameters is estimated to be $\sim 0.6\%$, while the uncertainties due to the errors of the $\psi(3770)$ and $\psi(2S)$ resonance parameters are estimated to be $\sim 1.5\%$ and $\sim 1.2\%$, respectively. Combining these uncertainties in quadrature yields the systematic uncertainty in the efficiency ϵ_{had} to be about 2%.

The second column of table IV lists the efficiencies for detection of the inclusive hadronic events at three energy points in the case of setting the continuum R value to be at 2.26 (see section IV).

D. Trigger efficiency

The requirements of the trigger for recording the data on-line are almost the same as those used in collecting the

TABLE IV: Summary of the efficiencies for detection of the inclusive hadronic events and the observed cross sections for $e^+e^- \to hadrons$ at three energy points, where the error in $\epsilon_{\rm had}$ is statistical only; while the errors in $\sigma^{\rm obs}_{\rm had}$ are statistical and point-to-point systematic, respectively.

E_{cm} (GeV)	$\epsilon_{\rm had}$	$\sigma^{\rm obs}_{\rm had}$ (nb)
3.650	0.4977 ± 0.0022	$18.983 \pm 0.087 \pm 0.182$
3.6648	0.5033 ± 0.0023	$18.299 \pm 0.199 \pm 0.176$
3.773	0.5528 ± 0.0022	$27.680 \pm 0.056 \pm 0.266$

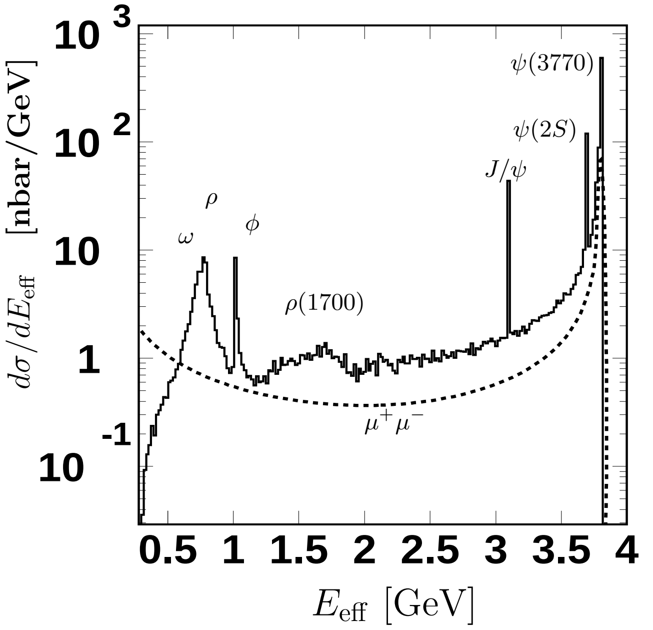

FIG. 4: The differential cross section for the inclusive hadronic event production when setting the nominal c.m. energy to be at 3.80 GeV; the histogram shows the resonances and continuum hadronic event production; the dashed line shows the cross sections for $\mu^+\mu^-$ pair production.

data for the work [16] and the work [17]. However, for the $\psi(3770)$ data acquisition, we slightly modified the trigger requirements for the charged tracks, which results in a little bit improvement in recording the two charged trak events. The trigger efficiencies are obtained by comparing the responses to different trigger requirements in the data taken at 3.097 GeV during the time period taking the data at $\sqrt{s} = 3.773$ GeV. The trigger efficiencies are measured to be 100.0% for both the $e^+e^- \to (\gamma)e^+e^-$ and $e^+e^- \to hadrons$ events, with an uncertainty of $^{+0.0}_{-0.5}$%.

E. Observed hadronic event cross sections

The observed cross section for inclusive hadronic event production can be obtained from Eq. (3) substituting $N_{\rm had}(E_{{\rm cm},i})$ with $N^{\rm zfit}_{\rm had} - N_b$, where N_b is the number of the background events, such as $e^+e^- \to \tau^+\tau^-$, $e^+e^- \to (\gamma)e^+e^-$, $e^+e^- \to (\gamma)\mu^+\mu^-$ and two-photon exchange processes. The number of the background events can be estimated by using the theoretical cross sections of these processes, the rates of misidentifying these processes as hadronic events and the total integrated luminosities of the data sets, which is given by

$$\begin{aligned} N_b \;=\; & L \times (\eta_{l^+l^-}\sigma_{l^+l^-} + \eta_{e^+e^-l^+l^-}\sigma_{e^+e^-l^+l^-} \\ & + \eta_{e^+e^-\pi^+\pi^-}\sigma_{e^+e^-\pi^+\pi^-} \\ & + \eta_{e^+e^-hadrons}\sigma_{e^+e^-hadrons}), \end{aligned} \qquad (5)$$

where $\sigma_{l^+l^-}$, $\sigma_{e^+e^-l^+l^-}$, $\sigma_{e^+e^-\pi^+\pi^-}$ and $\sigma_{e^+e^-hadrons}$ are the cross sections for $e^+e^- \to l^+l^-$, $e^+e^- \to e^+e^-l^+l^-$, $e^+e^- \to e^+e^-\pi^+\pi^-$, and $e^+e^- \to e^+e^-hadrons$ processes, respectively; while $\eta_{l^+l^-}$, $\eta_{e^+e^-l^+l^-}$, $\eta_{e^+e^-\pi^+\pi^-}$, and $\eta_{e^+e^-hadrons}$ are the corresponding misidentification rates.

In the calculation of the $\tau^+\tau^-$ cross section, we consider the contributions from $\psi(2S)$ decay, the QED production and their interference; we also consider the effects of the initial and final state radiative corrections and Coulomb interaction on the cross section [18]. For $e^+e^- \to (\gamma)e^+e^-$ [8], $e^+e^- \to (\gamma)\mu^+\mu^-$ [19] and two-photon processes $e^+e^- \to e^+e^-l^+l^-$ [20], the cross sections are read from respective generator outputs. As for the estimate of the total cross section for $e^+e^- \to e^+e^-hadrons$, we employ the equivalent photon approximation formalisms to deal with the γ-γ collision subprocess [21] [22]. In the sub-process, the energy dependence of the total hadronic cross section can be described well by the formula of Donnachie-Landshoff parameterization [23] above the three pion threshold. For the contribution in the low energy region below the three pion threshold, it is good enough to use the simple point-like $\pi^+\pi^-$ production cross section in the calculation [21].

The rates of misidentifying the above processes as the hadronic events are obtained from Monte Carlo simulation with the generators mentioned above. For the two-photon process $e^+e^- \to e^+e^-hadrons$, we use the Monte Calro generator described in [20] to simulate the process and determine the rates of misidentifying the processes as the hadronic events. The fourth and fifth columns of Table I give the estimated numbers ($n_{l^+l^-}$, $n_{e^+e^-l^+l^-}$ and $n_{e^+e^-h}$) of the background events from the $e^+e^- \to l^+l^-$ and the two-photon exchange processes, which are misidentified as the inclusive hadronic events.

Inserting $N^{\rm zfit}_{\rm had}$, N_b, L, $\epsilon_{\rm had}$ and $\epsilon^{\rm trig}_{\rm had}$ in Eq. (3), we obtain the observed cross sections for the inclusive hadronic event production at each of the three energy points, which are summarized in table IV, where the first error is statistical and second point-to-point systematic error arising from the uncertainty in $\epsilon_{e^+e^-}$ (0.6%), uncertainty in $N_{e^+e^-}$ ($\sim (0.2 \sim 0.5\%)$) and uncertainty in $\epsilon_{\rm had}$ (0.5%). The common systematic uncertainty is not included yet.

IV. LOWEST ORDER CROSS SECTION

A. Radiative corrections

To get the lowest order cross section for the inclusive hadronic event production in e^+e^- annihilation, the observed cross section has to be corrected for the radiative effects including the initial state radiative corrections and the vacuum polarization corrections. The correction factor, $(1+\delta(s))$, is given by

$$(1+\delta(s)) = \frac{\sigma^{\rm exp}(s)}{\sigma^{\rm B}(s)}, \tag{6}$$

where $\sigma^{\rm exp}(s)$ is the expected cross section and $\sigma^{\rm B}(s)$ lowest order cross section for the inclusive hadronic event production.

The expected cross section for hadronic event production can be written as

$$\sigma^{\rm exp}(s) = \int_0^{1-\frac{4m^2_{\pi(D)}}{s}} dx \cdot \frac{\sigma^{\rm B}(s(1-x))}{|1-\Pi(s(1-x))|^2} F(x,s), \tag{7}$$

where $\sigma^{\rm B}(s(1-x))$ is the total lowest order cross section in the energy range from 0.28 GeV to $\sqrt{s}$ (or from 3.729 GeV to $\sqrt{s}$ in the case of considering the $D\bar{D}$ production), $F(x,s)$ is a sampling function and $\frac{1}{|1-\Pi(s(1-x))|^2}$ is the correction factor for the effects of vacuum polarization including both the leptonic and hadronic terms in QED [24], with

$$\Pi(s^{'}) = \Pi_{\rm had}(s^{'}) + \Pi_l(s^{'}), \tag{8}$$

the effects of hadronic vacuum polarization can be calculated via the dispersion integral [25]

$$\Pi_{\rm had}(s^{'}) = \frac{s^{'}}{4\pi^2\alpha}\left[{\rm PV}\int_{4m^2_\pi}^{\infty} \frac{\sigma^{\rm B}(s^{''})}{s^{'}-s^{''}} ds^{''} - i\pi\sigma^{\rm B}(s^{'})\right], \tag{9}$$

while

$$\Pi_l(s^{'}) = \frac{1}{2}\delta^{l^+l^-}_{vac}(s^{'}), \tag{10}$$

$$\delta^{l^+l^-}_{vac}(s^{'}) = \frac{2\alpha}{\pi} f(\xi), \tag{11}$$

$$f(\xi) = -\frac{5}{9} - \frac{\xi}{3} + \frac{\sqrt{1-\xi}(2+\xi)}{6} \ln\left[\frac{1+\sqrt{1-\xi}}{1-\sqrt{1-\xi}}\right], (\xi \le 1), \tag{12}$$

$$f(\xi) = -\frac{5}{9} - \frac{\xi}{3} + \frac{\sqrt{1-\xi}(2+\xi)}{3} \tan^{-1}\frac{1}{\sqrt{\xi-1}}, (\xi > 1), \tag{13}$$

with $\xi = \frac{4m_l^2}{s^{'}}$, where m_l is the lepton mass.

In the structure function approach by Kuraev and Fadin [24],

$$F(x,s) \ = \ \beta x^{\beta-1}\delta^{V+S} + \delta^H, \tag{14}$$

where β is the electron equivalent radiator thickness,

$$\beta \ = \ \frac{2\alpha}{\pi}\left(\ln\frac{s}{m_e^2} - 1\right), \tag{15}$$

$$\delta^{V+S} \ = \ 1 + \frac{3}{4}\beta + \frac{\alpha}{\pi}\left(\frac{\pi^2}{3} - \frac{1}{2}\right) - \frac{\beta^2}{24}\left(\frac{1}{3}\ln\frac{s}{m_e^2} + 2\pi^2 - \frac{37}{4}\right), \tag{16}$$

$$\delta^H \ = \ \delta^H_1 + \ \delta^H_2, \tag{17}$$

$$\delta^H_1 \ = \ -\beta\left(1 - \frac{x}{2}\right), \tag{18}$$

$$\delta^H_2 = \frac{1}{8}\beta^2\left[4(2-x)\ln\frac{1}{x} - \frac{1+3(1-x)^2}{x}\ln(1-x) - 6 + x\right]. \tag{19}$$

In above expressions, m_e is the mass of electron and α is the fine structure constant.

For the resonances, such as $\psi(2S)$, J/ψ, ϕ and ω, we use the Breit-Wigner formula

$$\sigma^{\rm B}(s^{'}) \ = \frac{12\pi\Gamma^0_{ee}\Gamma_h}{(s^{'}-M^2)^2 + \Gamma^2 M^2} \tag{20}$$

to calculate the lowest order cross section, where M and Γ are the mass and the total width of the resonance, and $\Gamma_{ee} = \Gamma^0_{ee}|1-\Pi(s^{'})|^{-2}$ and Γ_h are the partial widths to the e^+e^- channel and to the inclusive hadronic final state, respectively. For the $\psi(3770)$ resonance, we use

$$\sigma^{\rm B}(s^{'}) \ = \frac{12\pi\Gamma^0_{ee}\Gamma_{tot}(s^{'})}{(s^{'}-M^2)^2 + \Gamma^2_{tot}(s^{'})M^2} \tag{21}$$

to calculate the lowest order cross section, where $\Gamma_{\rm tot}(s^{'})$ is chosen to be energy dependent and normalized to the total width $\Gamma_{\rm tot}$ at the peak of the resonance. The $\Gamma_{\rm tot}(s^{'})$ is defined as

$$\Gamma_{\rm tot}(s^{'}) = \Gamma_{D^0\bar{D}^0}(s^{'}) + \Gamma_{D^+D^-}(s^{'}) + \Gamma_{non-D\bar{D}}(s^{'}), \tag{22}$$

where $\Gamma_{D^0\bar{D}^0}(s^{'})$, $\Gamma_{D^+D^-}(s^{'})$ and $\Gamma_{\rm non-D\bar{D}}(s^{'})$ are the partial widths for $\psi(3770) \to D^0\bar{D}^0$, $\psi(3770) \to D^+D^-$ and $\psi(3770) \to {\rm non}-D\bar{D}$, respectively, which are taken in the form

$$\Gamma_{D^0\bar{D}^0}(s^{'}) \ = \ \Gamma_0 \ \theta(E_{cm} - 2M_{D^0})\frac{(p_{D^0})^3}{(p^0_{D^0})^3}\frac{1+(rp_{D^00})^2}{1+(rp_{D^0})^2}B_{00}, \tag{23}$$

$$\Gamma_{D^+D^-}(s^{'}) \ = \ \Gamma_0 \ \theta(E_{cm} - 2M_{D^+}) \frac{(p_{D^+})^3}{(p^0_{D^+})^3} \frac{1 + (rp^0_{D^+})^2}{1 + (rp_{D^+})^2} B_{+-}, \tag{24}$$

and

$$\Gamma_{non-D\bar{D}}(s^{'}) = \Gamma_0 \ \left[1 - B_{00} - B_{+-}\right], \tag{25}$$

where p^0_D and p_D are the momenta of the D mesons produced at the peak of $\psi(3770)$ and at the c.m. energy $\sqrt{s'}$, respectively; Γ_0 is the total width of the $\psi(3770)$ at the peak, and r is the interaction radius of the $c\bar{c}$, which is set to be 1.0 fm; B_{00} and B_{+-} are the branching fractions for $\psi(3770) \to D^0\bar{D}^0$ and $\psi(3770) \to D^+D^-$, respectively; $\theta(E_{cm} - 2M_{D^0})$ and $\theta(E_{cm} - 2M_{D^+})$ are the step functions to account for the thresholds of the $D\bar{D}$ production.

In the calculation of the lowest order cross section, the $\psi(3770)$ resonance parameters $M = 3772.3 \pm 1.0$ MeV, $\Gamma_0 = 25.5 \pm 3.1$ MeV and $\Gamma_{ee} = 0.224 \pm 0.031$ keV measured by BES Collaboration [30] are used. Inserting the resonance parameters of J/ψ, $\psi(2S)$ quoted from PDG [26] and the $R = 2.26 \pm 0.14$ [6][16] for the light hadron production in the energy range from 2.0 to 3.0 GeV measured by BES Collaboration in Eqs. (6)–(25), we obtain the radiative correction factors at the three energy points, which are summarized in table V. In determination of the value of $(1 + \delta(s))$, the input of R value in calculating the cross section for continuum hadronic event production affects the value of $(1 + \delta(s))$. Varying the input R by ±10% causes a variation of ±1.3% in $(1 + \delta(s))$, which results in a variation of the product $\epsilon_{had}(1 + \delta(s))$ by only ±0.4%. The most uncontrolled cross sections in the calculation of $(1 + \delta(s))$ come from the hadronic cross sections in the energy range from 1.2 to 2.0 GeV. However, the whole contribution of the cross section from this energy range is less than 5% of the total observed cross section in our case. Since the efficiency is quite low for detection of the hadronic events from this energy range ($\epsilon_{had} < 10\%$), the amount of the product $\epsilon_{had}(1 + \delta(s))$ would also be rather stable with error less than 0.4%. Taking into account the uncertainty in the measured hadronic event production and the errors of the resonance parameters together, the total uncertainty in R measurement due to the calculation of $(1 + \delta(s))$ is then estimated to be less than 1.5% in this work.

B. Lowest order cross sections and R values

The lowest order cross section for inclusive hadronic event production is obtained by

$$\sigma^{\rm B}_h(s) = \frac{\sigma^{\rm obs}_{\rm h}(s)}{(1 + \delta(s))}, \tag{26}$$

where

$$\sigma^{\rm B}_h(s) = \sigma^{\rm B}_{e^+e^- \to hadrons}(s) + \sum \sigma^{\rm B}_{{\rm Res},i}(s), \tag{27}$$

in which $\sigma^{\rm B}_{e^+e^- \to hadrons}(s)$ is the cross section for inclusive hadronic event production through one photon annihilation, $\sigma^{\rm B}_{{\rm Res},i}(s)$ is the cross section for the ith resonance, such as J/ψ, $\psi(2S)$, $\psi(3770)$ etc. which decays into hadronic final states.

To obtain the lowest order cross section $\sigma^0_{\rm h}(s) = R_{uds} \cdot \sigma^{\rm B}_{\mu^+\mu^-}(s) = \sigma^{\rm B}_{e^+e^- \to hadrons}(s)$ for the hadronic event production through one photon annihilation at the energies of 3.650 and 3.6648 GeV, and the lowest order cross section $\sigma^0_{\rm h}(s) = (R_{uds} + R_{\psi(3770)}) \cdot \sigma^B_{\mu^+\mu^-} = \sigma^{\rm B}_{e^+e^- \to hadrons}(s) + \sigma^{\rm B}_{\psi(3770)}(s)$ for both one photon annihilation and $\psi(3770)$ production at 3.773 GeV, the amount of the cross section due to the resonance production at the energies of 3.650 and 3.6648 GeV, and the amount of the cross section due to the resonance production but $\psi(3770)$ at 3.773 GeV have to be subtracted out. The third column of table V summarizes the lowest order cross sections $\sigma^0_{\rm h}(s)$. Dividing the $\sigma^0_{\rm h}(s)$ by the lowest order cross section for $\mu^+\mu^-$ production at the same c.m. energy, we obtain the R values, which are summarized in the fourth column of the table. The first error in the measured lowest order cross section and the R value listed in table V is statistical, the second is the point-to-point systematic and the third is common systematic error.

The common systematic error arises from the uncertainty in luminosity (∼ 1.8%), in selection of hadronic event (∼ 2.5%), in Monte Carlo Modeling (∼ 2.0%), in radiative correction (∼ 1.5%) for the measured cross sections and R values at the three energy points, and the uncertainty in $\psi(3770)$ resonance parameters (∼ 2.7%) for those at 3.773 GeV only. Adding these uncertainties in quadrature yields the total systematic uncertainties to be ∼ 4.0% and ∼ 4.9% for the measured hadronic cross sections and R values for the data taken below the $D\bar{D}$ threshold and at 3.773 GeV, respectively.

Averaging the R values measured at the first two energy points (3.650 and 3.6648 GeV) by weighting the combined statistical and point-to-point systematic errors, we obtain

$$\bar{R}_{uds} = 2.224 \pm 0.019 \pm 0.089,$$

where the first error is combined from statistical and point-to-point systematic errors, and the second is common systematic. This $\bar{R}_{uds}$ excludes the contribution from resonances and reflects the lowest order cross section for the inclusive light hadronic event production through one photon annihilation of e^+e^-. So it can be directly compared with those calculated based on the pQCD. The value is consistent with $\bar{R}_{uds} = 2.26 \pm 0.14$ obtained by fitting those [12] measured in the energy region between 2.0 and 3.0 GeV [6] and with $\bar{R}_{uds} = 2.21 \pm 0.13$ obtained from fitting to the inclusive hadronic cross sections for both the $\psi(2S)$ and $\psi(3770)$ resonances in the energy region from 3.666 to 3.897 GeV [30].

Figure 5 displays the values of R from this measurement and previous measurements by BES Collabora-

TABLE V: Summary of the radiative correction factors, the lowest order cross sections and the R values measured at three energy points.

Energy (GeV)	$(1+\delta(s))$	$\sigma^0_{\rm h}(s)$ (nb)	R
3.6500	1.287	$14.624 \pm 0.067 \pm 0.142 \pm 0.590$	$2.243 \pm 0.010 \pm 0.022 \pm 0.090$
3.6648	1.261	$14.151 \pm 0.158 \pm 0.139 \pm 0.580$	$2.188 \pm 0.024 \pm 0.022 \pm 0.088$
3.7730	1.195	$23.142 \pm 0.047 \pm 0.222 \pm 1.158$	$3.793 \pm 0.008 \pm 0.036 \pm 0.190$

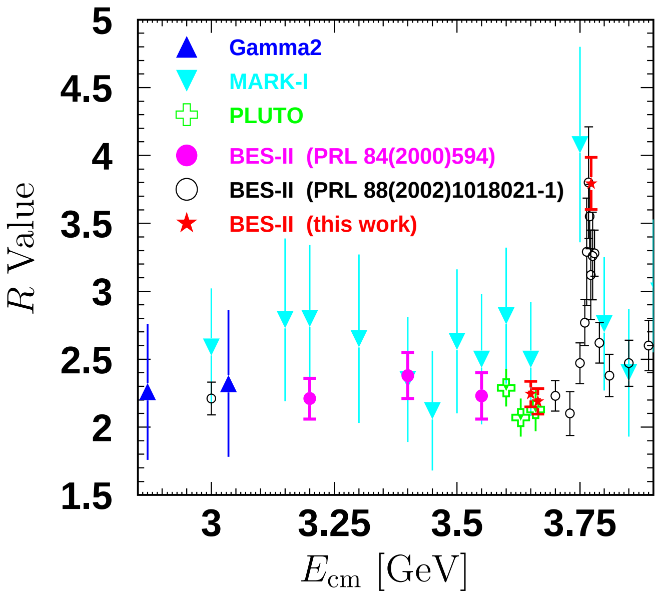

FIG. 5: The values of R measured by BES Collaboration, MARK-I Collaboration, $\gamma\gamma 2$ Collaboration and PLUTO Collaboration in the energy region between 2.85 and 3.90 GeV, where the error bars show the combined statistical and systematic errors in quadrature.

tion [12] [16], MARK-I Collaboration [27], $\gamma\gamma 2$ Collaboration [28] and PLUTO Collaboration [29] in the energy region between 2.85 and 3.90 GeV. The error bars shown in the figure are obtained by combining statistical and systematic errors in quadrature.

Using the measured R value at 3.773 GeV listed in table V and the $\bar{R}_{uds}$ value for light hadron production measured below the $D\bar{D}$ threshold we obtain the $R_{\psi(3770)}$ due to $\psi(3770)$ decays to be

$$R_{\psi(3770)} = 1.569 \pm 0.042 \pm 0.133, \qquad (28)$$

where the first error is combined from statistical and point-to-point systematic error and the second common systematic. In estimation of the systematic uncertainty, we assumed that the same amount of the systematic uncertainties in the measured values of the R and the $\bar{R}_{uds}$ is canceled in subtracting the $\bar{R}_{uds}$ from the R. The corresponding lowest order cross section for $\psi(3770)$ production is

$$\sigma^{\rm B}_{\psi(3770)} = (9.575 \pm 0.256 \pm 0.813) \quad \text{nb}. \qquad (29)$$

V. BRANCHING FRACTIONS FOR THE DECAYS $\psi(3770) \to D^0\bar{D}^0, D^+D^-, D\bar{D}$ AND FOR $\psi(3770) \to {\rm non}-D\bar{D}$

Assuming that there are no other new structure and effects except the $\psi(3770)$ resonance and the continuum hadron production in the energy region from 3.70 GeV to 3.86 GeV, the branching fraction for $\psi(3770) \to D\bar{D}$ can be determined by

$$BF(\psi(3770) \to D\bar{D}) = \frac{\sigma^{\rm obs}_{D\bar{D}}}{(1+\delta)_{D\bar{D}}\ \sigma^{\rm B}_{\psi(3770)}}, \qquad (30)$$

where $\sigma^{\rm obs}_{D\bar{D}}$ and $\sigma^{\rm B}_{\psi(3770)}$ are the observed and lowest order production cross sections for $D\bar{D}$ and inclusive hadronic events, respectively; $(1+\delta)_{D\bar{D}}$ is the radiative correction factor for $D\bar{D}$ production. Inserting the $\psi(3770)$ resonance parameters ($M = 3772.3 \pm 1.0$ MeV; $\Gamma_{\rm tot} = 25.5 \pm 3.1$ MeV and $\Gamma_{ee} = 0.224 \pm 0.031$ keV) measured by BES Collaboration [30] in Eqs. (6) and (7) with combining the Eqs. (7)-(25) together, we obtain the radiative correction factor

$$(1+\delta)_{D\bar{D}} = 0.764 \pm 0.014, \qquad (31)$$

where the error is the uncertainty arising from the errors of the $\psi(3770)$ resonance parameters, the uncertainty in vacuum polarization correction and the uncertainty arising from varying the branching fraction for $\psi(3770) \to D\bar{D}$ from 84% to 100%.

BES Collaboration measured the observed cross sections for $D^0\bar{D}^0$ and D^+D^- production at c.m. energy $\sqrt{s} = 3.773$ GeV to be $\sigma_{D^0\bar{D}^0} = (3.58 \pm 0.09 \pm 0.31)$ nb and $\sigma_{D^+D^-} = (2.56 \pm 0.08 \pm 0.26)$ nb [6]. These observed cross sections were obtained by analyzing the same data set from which the R value at $\sqrt{s} = 3.773$ GeV is measured.

Inserting the $\sigma^{\rm B}_{\psi(3770)}$, the observed cross sections for $D^0\bar{D}^0$, D^+D^-, $D\bar{D}$ production at 3.773 GeV and the radiative correction factor, $(1+\delta)_{D\bar{D}}$, in Eq. (30), we obtain the branching fractions for the decays $\psi(3770) \to D^0\bar{D}^0, D^+D^-, D\bar{D}$ to be

$$BF(\psi(3770) \to D^0\bar{D}^0) = (48.9 \pm 1.2 \pm 3.8)\%, \qquad (32)$$

$$BF(\psi(3770) \to D^+D^-) = (35.0 \pm 1.1 \pm 3.3)\%, \qquad (33)$$

and

$$BF(\psi(3770) \to D\bar{D}) = (83.9 \pm 1.6 \pm 5.7)\%, \qquad (34)$$

which results in the non-$D\bar{D}$ branching fraction of $\psi(3770)$ to be

$$BF(\psi(3770) \to {\rm non}-D\bar{D}) = (16.1 \pm 1.6 \pm 5.7)\%, \qquad (35)$$

TABLE VI: Sources of the uncanceled systematic uncertainties in the measured cross sections for $D\bar{D}$ and $\psi(3770)$ production, where upper ^{N} and upper ^{C} mean the uncertainties for the neutral mode $D^0\bar{D}^0$ and the charged mode D^+D^-, respectively; for the uncertainties in the measured cross section for $D\bar{D}$ production, please refer to the reference [6]; we here re-estimate the uncertainty in the combined tracking and kinematic fit in selection of D events to be $\sim 4.0\%$.

Source	$\frac{\Delta\sigma^{\rm obs}_{D\bar{D}}}{\sigma^{\rm obs}_{D\bar{D}}}$ [%]	Source	$\frac{\Delta\sigma_{\psi(3770)}}{\sigma_{\psi(3770)}}$ [%]
Particle ID	~ 1.5	Monte Carlo Modeling	~ 2.0
Tracking & K.F.	~ 4.0	Hadron selection	~ 2.5
F. P.	~ 3.0		
MC Statistics	~ 0.6		
Br for D^0	~ 3.2		
(Br for D^+)	(~ 6.5)		
Total	$\sim 6.2\ ^N$ $(\sim 8.4)\ ^C$	Total	~ 3.2

where the first error is statistical and the second systematic arising from uncanceled systematic uncertainties. The uncanceled relative systematic uncertainties are $\sim 6.2\%$, $\sim 8.4\%$ and $\sim 3.2\%$ for the $\sigma^{\rm obs}_{D^0\bar{D}^0}$, $\sigma^{\rm obs}_{D^+D^-}$ and the $\sigma^{\rm B}_{\psi(3770)}$, respectively. The systematic error also includes the common uncertainty of $\sim 2.7\%$ arising from the statistical uncertainty in the measured lowest order cross section for $\psi(3770)$ production and the uncertainty ($\sim 1.8\%$) in radiative correction factor $(1+\delta)_{D\bar{D}}$. Table VI summarizes sources of the uncanceled systematic uncertainties for the measured $\sigma^{\rm obs}_{D\bar{D}}$ and $\sigma_{\psi(3770)}$. The uncertainties in luminosity ($\sim 1.8\%$), in $\psi(3770)$ resonance parameters ($\sim 2.7\%$) and in radiative correction ($\sim 1.5\%$) are canceled out in the estimation of the systematic uncertainty in the measured branching fractions.

VI. DISCUSSION ABOUT INTERFERENCE EFFECTS

TABLE VII: Summary of the radiative correction factors, the lowest order cross sections and the R values measured at three energy points, where the interference effects between the $\psi(2S)$ electromagnetic decays and hadron production through non-resonant annihilation of e^+e^- are taken into account.

Energy (GeV)	$(1+\delta(s))$	$\sigma^{0\ \rm crr}_{\rm h}(s)$ (nb)	R
3.6500	1.300	$14.855 \pm 0.067 \pm 0.140 \pm 0.584$	$2.279 \pm 0.010 \pm 0.022 \pm 0.089$
3.6648	1.285	$14.543 \pm 0.155 \pm 0.137 \pm 0.570$	$2.249 \pm 0.024 \pm 0.021 \pm 0.086$
3.7730	1.198	$22.951 \pm 0.047 \pm 0.222 \pm 1.155$	$3.762 \pm 0.008 \pm 0.036 \pm 0.189$

The measured R values discussed in above sections are obtained based on the same treatment on the measurements of inclusive hadronic cross sections in which no interference between the inclusive hadronic final states of the resonance decays and the inclusive hadronic final states from non-resonance annihilation of e^+e^- is taken into account [12][16][31]. However, since the c.m. energies of 3.650 GeV, 3.6648 GeV and 3.773 GeV are close to the $\psi(2S)$ resonance, there may be interference effects between the final hadronic states from the $\psi(2S)$ electromagnetic decays and the continuum hadron production in annihilation of e^+e^-. These interference effects distort the line shape of the continuum hadron production cross section around the $\psi(2S)$ peak. With the definition of the R given in Eq. (2), we can estimate the destructive/constructive amount of the cross section due to the interference effects, which is given by

$$\sigma^{\rm interf}_{\rm had} = R\ \sigma^{\rm interf}_{\mu^+\mu^-}. \tag{36}$$

The destructive/constructive amounts of the cross sections given in R are estimated to be -0.0581, -0.1026 and $+0.0219$ at 3.650 GeV, 3.6648 GeV and 3.773 GeV, respectively. After correcting the cross section $\sigma^0_h(s)$ for the destructive/constructive amounts due to the interference effects, we obtained the lowest order cross section $\sigma^{0\ \rm crr}_{\rm h}(s)$. The third column of table VII summarizes the $\sigma^{0\ \rm crr}_{\rm h}(s)$. In the case of considering the interference effects, the correction factor $(1+\delta(s))$ is also changed. The second column of table VII lists the correction factor at the c.m. energies. Dividing the $\sigma^{0\ \rm crr}_{\rm h}(s)$ by the lowest order cross section for $\mu^+\mu^-$ production at the same c.m. energy, we obtain the R values, which are summarized in the fourth column of the table. The errors are statistical, the point-to-point systematic and the common systematic as discussed before.

The weighted average of the R values measured at the first two energy points is

$$\bar{R}_{uds} = 2.268 \pm 0.019 \pm 0.091,$$

where the first error is combined from statistical and point-to-point systematic errors, and the second is common systematic.

Following the same procedure as discussed in Sections IV and Section V, we obtained the lowest order cross section for $\psi(3770)$ production to be

$$\sigma^{\rm B}_{\psi(3770)} = (9.113 \pm 0.255 \pm 0.805) \quad {\rm nb}, \tag{37}$$

and the branching fractions for $\psi(3770)$ decays to be

$$BF(\psi(3770) \to D^0\bar{D}^0) = (51.4 \pm 1.3 \pm 4.0)\%, \tag{38}$$

$$BF(\psi(3770) \to D^+D^-) = (36.8 \pm 1.1 \pm 3.5)\%, \tag{39}$$

$$BF(\psi(3770) \to D\bar{D}) = (88.2 \pm 1.7 \pm 6.0)\%, \tag{40}$$

and

$$BF(\psi(3770) \to \mathrm{non}-D\bar{D}) = (11.8 \pm 1.7 \pm 6.0)\%, \quad (41)$$

where the errors are statistical and the systematic arising from some uncanceled systematic uncertainties.

VII. SUMMARY

From the analysis of the data taken at 3.650, 3.6648 and 3.773 GeV in e^+e^- annihilation, we measured the R values at the energy points, which are $R = 3.793 \pm 0.037 \pm 0.190$ at 3.773 GeV and $\bar{R}_{uds} = 2.224 \pm 0.019 \pm 0.089$ at $\sqrt{s}$ below the $D\bar{D}$ threshold. Based on the measured R values, we determined the lowest order cross section for $\psi(3770)$ production at 3.773 GeV to be $\sigma^{\mathrm{B}}_{\psi(3770)} = (9.575 \pm 0.256 \pm 0.813)$ nb, the branching fractions for $\psi(3770)$ decays to be $BF(\psi(3770) \to D^0\bar{D}^0) = (48.9 \pm 1.2 \pm 3.8)\%$, $BF(\psi(3770) \to D^+D^-) = (35.0 \pm 1.1 \pm 3.3)\%$ and $BF(\psi(3770) \to D\bar{D}) = (83.9 \pm 1.6 \pm 5.7)\%$, which result in the non-$D\bar{D}$ branching fraction of $\psi(3770)$ to be $BF(\psi(3770) \to \mathrm{non}-D\bar{D}) = (16.1 \pm 1.6 \pm 5.7)\%$. These branching fractions for $\psi(3770)$ decays are measured for the first time.

ACKNOWLEDGEMENTS

The BES collaboration thanks the staff of BEPC for their hard efforts. This work is supported in part by the National Natural Science Foundation of China under contracts Nos. 19991480,10225524,10225525, the Chinese Academy of Sciences under contract No. KJ 95T-03, the 100 Talents Program of CAS under Contract Nos. U-11, U-24, U-25, and the Knowledge Innovation Project of CAS under Contract Nos. U-602, U-34(IHEP); by the National Natural Science Foundation of China under Contract No.10175060(USTC),and No.10225522(Tsinghua University).

[1] N. Cabibbo, R. Gatto, Phys. Rev. 124 (1961) 1577; H. Burkhardt, F. Jegerlehner, G. Penso, C. Verzegnassi, Z. Phys. **C 43** (1989) 497; G. Altarelli, CERN-TH73194/94; A.D. Martin, D. Zeppenfeld, Phys. Lett. **B 345** (1995) 558; M. Davier, S Eidelman, A. Hocker, Z. Zhang, Eur. Phys. J. **C 27** (2003)497.
[2] W. Bacino *et al.* (DELCO Collaboration), Phys. Rev. Lett. **40** (1978) 671.
[3] J.Z. Bai *et al.* (BES Collaboration), HEP&NP **28** (2004) 325.
[4] J.Z. Bai *et al.* (BES Collaboration), Phys. Lett. **B 605** (2005) 63.
[5] N.E. Adam *et al.* (CLEO Collaboration), Phys. Rev. Lett. **96** (2006) 082004; T.E. Coan *et al.* (CLEO Collaboration), Phys. Rev. Lett. **96** (2006) 182002
[6] J.Z. Bai *et al.* (BES Collaboration), Phys. Lett. **B 603** (2004) 130.
[7] J.Z. Bai *et al.* (BES Collaboration), Nucl. Instrum. Methods **A 458** (2001) 627.
[8] The generator was written by R. Kleiss *et al.*. based on: F.A. Berends, et al, Nucl. Phys. **B 228** (1983) 537
[9] D. Zhang, G. Rong and J.C. Chen, arXiv:hep-ph/0604264.
[10] M. Ablikim *et al.* (BES Collaboration), Nucl. Instr. and Meth. **A. 552** (2005) 344, arXiv:physics/0503001.
[11] T. Sjostrand, Comput. Phys. Commun., **82** (1994) 74.
[12] J.Z. Bai *et al.* (BES Collaboration), Phys. Rev. Lett. **84** (2000) 594.
[13] J.C. Chen *et al.*, Phys. Rev. **D 62** (2000) 034003.
[14] R.R. Akhmetshin, *et al.*, (CMD-2 Collaboration), Phys. Lett. **B 578** (2004) 285.
[15] G. Gounaris and J.Sakurai, Phys. Rev. Lett. **21** (1968) 244.
[16] J.Z. Bai *et al.* (BES Collaboration), Phys. Rev. Lett. **88** (2002) 101802.
[17] J.Z. Bai *et al.* (BES Collaboration), Phys. Lett. **B 550** (2002) 24.
[18] J.Z. Bai, *et al.* (BES Collaboration), Phys. Rev. **D 53** (1996) 20.
[19] The generator was written by S. Van der Mark based on: F.A. Berends *et al.*, Nucl. Phys. **B 57** (1973) 381.
[20] F.A. Berends, P.H. Daverveldt and R. Kleiss, Comput. Phys. Commun., **40** (1986) 285.
[21] S.J. Brodsky, T. Kinoshita and H. Terazawa, Phys. Rev. **D 4** (1971) 1532.
[22] D. Morgan, M.R. Pennington and M.R. Whalley, J. Phys. G20 Suppl. 8A (1994) A1.
[23] A. Donnachie and P.V. Landshoff, Phys. Lett. **B 296** (1992) 227.
[24] E. A. Kuraev and V. S. Fadin, Yad Fiz. **41**, 733 (1985); [Sov. J. Nucl. Phys. **41** (1985) 466].
[25] F.A. Berends and G.J. Komen, Phys. Lett. **B 63** (1976) 432; A.B. Arbuzov, E.A. Kuraev *et al.*, JHEP10 (1997) 006.
[26] S. Eidelman *et al.* (Particle Data Group), Phys. Lett. **B 592** (2004) 1.
[27] J.L. Siegrist, *et al.* (MARK-I Collaboration), Phys. Rev. D **26** (1982) 969.
[28] C. Bacci, *et al.* ($\gamma\gamma 2$ Collaboration), Phys. Lett. **B 86** (1979) 234.
[29] L. Criegee and G. Knies, Phys. Rep. **83** (1982) 151; J. Burmester *et al.* (PLUTO Collaboration), Phys. Lett. **B 66** (1977) 395.
[30] M. Ablikim *et al.* (BES Collaboration), Contribution paper to Lepton Photon 2005 (LP05-452); Gang RONG (for BES Collaboration), Proceedings of the 32nd International Conference on High Energy Physics, Beijing, China, 16-22 August 2004.
[31] A.M. Boyarski *et al.* (MARK-I Collaboration), Phys. Rev. Lett. **34** (1975) 1357; V. Luth *et al.* (MARK-I Collaboration), Phys. Rev. Lett. **35** (1975) 1124; J.Z. Bai *et al.* (BES Collaboration), Phys. Lett. **B** 355 (1995) 374; J.Z. Bai *et al.* (BES Collaboration), Phys. Lett. **B** 550 (2004) 24.